SSS-R-77-3048

**FE-1770-19**
**Distribution Category UC-90c**

# COMPUTER MODELING OF COAL GASIFICATION REACTORS

Quarterly Technical Progress Report
For Period June 1, 1976 — September 30, 1976

Thomas R. Blake

Systems, Science and Software
La Jolla, California 92038

October 1976

PREPARED FOR
ENERGY RESEARCH AND DEVELOPMENT ADMINISTRATION

Under Contract No. E(49-18)-1770

---

# TABLE OF CONTENTS

# ABSTRACT

This report presents a summary of the work accomplished during the fifth quarter of a three year study conducted for the U.S. Energy Research and Development Administration under Contract No. E(49-18)-1770. The objective of this research is to develop and apply computer codes, based upon continuum theories of multiphase, reactive flows, to the performance of fluidized bed and entrained flow reactors for coal gasification.

# I. OBJECTIVE AND SCOPE OF WORK

The purpose of this program is to develop and apply, over three years, general computer models that will expedite the development and aid in the optimization and scale-up of reactors for coal gasification. Initial applications will be to fluidized bed gasification processes; subsequently both entrained flow reactors and fast fluidized beds will be examined.

During the first year, work will be initiated on the fluidized bed model in the areas of multiphase fluid flow without chemical reactions, and chemical reactions without fluid flow. The computer codes, developed to represent these aspects of gasification processes, will be combined in the second year of the program into a numerical model of reactive flows in fluidized beds. This model will provide a time-dependent field description of fluidized bed flows in two space dimensions. Calculations will be performed with the prototype code during the first and second years to verify the accuracy of the formulations employed and, in the second year, these calculations should provide preliminary results relevant to coal gasification. During the second year a computer model for entrained flow gasifiers will be formulated and the chemistry defined; this model will provide a field description of entrained flows in two space dimensions. Nonreactive flow calculations will be performed for entrained flow processes at the end of the second year.

In the third year the application of the fluidized bed computer model to specific gasifier processes will be extended and a computational model which includes three-dimensional effects will be developed. Also, during this third year the coal chemistry will be combined with the entrained flow computer model and some calculations of such gasifier configurations will be performed.

## II. SUMMARY OF PROGRESS TO DATE

This was the first quarter in the second year of this research to develop and apply computer codes, based upon continuum theories of multiphase flows, to the performance of fluidized bed and entrained flow reactors for coal gasification. Research was active in several areas.

In brief, the research related to the fluidized bed computer code included minor modifications to the two-dimensional thermohydrodynamic numerical model, continued formulations of constitutive equations and interaction functions for solid particle-gas flows and formulations of single particle-gas heterogeneous reaction models. A major revision of a homogeneous chemical reactor model to represent transient, constant volume, isothermal reactors was made and this homogeneous reactor model was used to study chemical parameter optimization.

The work on the entrained flow computer model was primarily directed to a review and summary of existing theoretical and experimental studies on entrained flow gasification and to the initial formulation of the conservation equations for multidimensional entrained flows.

# III. DETAILED DESCRIPTION OF TECHNICAL PROGRESS

## 3.1 TASK 00 — MANAGEMENT, DOCUMENTATION AND CONSULTING

The annual report, documenting the first year of research in the present contract, was prepared and submitted for review. This report has subsequently been approved for publication. In addition, at the end of June, 1976 we presented a review of the project to staff members of the Energy Research and Development Administration.

A paper, "A Numerical Model of Gas Fluidized Beds," has been accepted for presentation at the Annual A.I.Ch.E. meeting, Chicago, November 28. In this paper we discuss the nature of the theoretical formulation and the numerical model for two-dimensional flows in fluidized beds.

A presentation was given at the Electric Power Research Institute in July. In that talk we examined the nature of the first year of research in the present contract and subsequently discussed the application of such computer models to problems of interest in coal gasification.

In August, an ERDA/NSF/EPRI-sponsored symposium on coal chemistry was attended at the Stanford Research Institute.

Dr. S. K. Garg, while attending an IUTAM symposium in Europe, visited with Rietema and Musters, in the former's laboratory. Rietema's experimental work was used extensively in some of our fluidized bed model formulations (c.f. our annual report[1]) and we continue to receive important data from that group.

Professor I. J. Siekmann of the Technische Hochschule, Darmstadt, spent one month at $S^3$ during August and September, consulting on this contract. In this visit, Professor Siekmann worked with Drs. Garg and Blake on formulations of the governing differential equations and constitutive equations for gas fluidized beds, particularly related to shear and bulk viscosity effects. He will continue, in Germany and in subsequent visits, his collaboration with $S^3$ on both fluidized bed and entrained flow modeling. Further, he has and will provide a ready communication with fluidized bed research in Europe.

Professor C. Y. Wen of West Virginia University provided, through telephone and mail communication, experimental measurements of flows in two-dimensional fluidized beds.

These measurements, in the form of motion picture records, are being compared with numerical calculations. Professor Wen visited $S^3$ for two days, September 20-21, and joined in technical planning discussions related to the task objectives in the second year of contract research. In addition to examinations of chemistry data, fluidized bed measurements and specific developments related to the numerical models, it was decided that Professor Wen would play a major role in the development of the chemistry model for steam-oxygen gasification processes. The administrative (e.g., contractual, scheduling) and technical (specific tasks) details of this activity will be formalized in October and November.

Professor Paul A. Libby of the University of California, San Diego, consulted with $S^3$ staff members on the subject of turbulence models and the relationship between the spatial mathematical averages in multiphase flows and those appropriate to turbulent models. Professor Libby is examining both the nature of possible turbulent stress formulations and also the coupling of the particle motion to the turbulent field for the entrained flow gasifier model.

## 3.2 TASK 02 – FLUIDIZED BED COAL GASIFICATION MODEL

The research on the fluidized bed model was directed to the further development of the chemistry and thermohydrodynamic computer models and to the theoretical formulations required for the incorporation of coal chemistry into thermohydrodynamic code. Again, during the first year of this contract, separate chemistry and thermohydrodynamic computer codes were developed.[1] The latter code provides a field description, in two spatial dimensions, of time-dependent nonreactive flow in gas fluidized beds. This code has been used to calculate the evolution of bubbles and solid particle convection in planar, two-dimensional beds with relatively simple geometric configurations. Qualitative agreement between the calculations and published data has been observed.[1] The chemistry code represented a homogeneous isothermal reactor; in the first year this code was developed with that chemistry necessary to describe the $CO_2$ Acceptor process. Time-dependent calculations, to steady state, were performed with this code and good agreement was obtained between those calculations and data from the pilot plant at Rapid City.[1] A major effort in the second year of this contract is to combine the chemistry with the thermohydrodynamic model, and to include in this chemistry, the reactions associated with steam-oxygen gasification processes (e.g., Synthane). To this end the basic thermohydrodynamic code is to be modified. Additional code development on homogeneous chemical reactor models is being conducted to provide a chemical kinetics code which can serve both as a testing device for the necessary chemistry and also to develop some numerical formulations which will be used directly in the combined chemistry-thermohydrodynamic mode. Further, we are formulating models for heterogeneous solid-gas reactions which include the mechanisms of extraparticle diffusion, interphase mass transport and intraparticle diffusion. Such formulations are necessary to define the source functions (mass, momentum and energy) which together with the chemistry must be included in the thermohydrodynamic model to account for chemically reactive flows. In the following paragraphs we briefly review the research related to these developments.

## Thermohydrodynamic Code

Some minor modifications were made in the two-dimensional thermohydrodynamic code; these changes relate to the description of solid particle convection. In the second quarter of this second year we expect to perform calculations with this code to model several fluidized bed configurations and thereby extend the calculational results reported during the first year of this contract. These calculations, which will be reported in the next quarterly report, involve the influences of bed height/width ratio, fluidized bed operating pressure, gas flow rate and inlet distribution of gas flow. While some of these calculations are for the evaluation of code capabilities, a major reason for this computational activity is to provide preliminary parametric data related to realistic systems.

Work continued on the formulation of the mechanical interaction functions for particle-particle and particle-gas momentum exchange. In particular, Professor Siekmann has suggested the incorporation of some additional data in our correlations of shear viscosity for the solid phase. Further, Rietema has communicated new measurements which can be useful in our correlation of elastic modulus for the solid phase. A theoretical formulation for the solid phase bulk viscosity is desirable; initial efforts to develop such a formulation have begun. Such a theoretical description of the bulk viscosity is useful because there are no experimental definitions of this quantity (c.f. [1]). In our initial studies we have been primarily concerned with obtaining some order of magnitude relationships between the bulk, $\lambda^s$, and shear, $\mu^s$, viscosities for the solid. Consequently, we have explored the analogy between momentum transport in moderately dilute solid particle distributions in fluidized environments and momentum transport in dilute and dense gases. With such a model we have established, in an asymptotic sense, the relationship between $\lambda^s$ and $\mu^s$ as the solid particle cloud density becomes that of a densely packed cloud. While such a model requires further study and, if possible, a more specific treatment of particle-particle interactions, it does provide valuable insight into the evaluation of $\lambda^s$. The analysis is presented in Appendix A.

The formulation of the model to represent heterogeneous solid gas reactions for a single particle was initiated (c.f. [7]-[9]). This model, when integrated over many particles, will lead to the source terms in the conservation equations of the fully interactive thermohydrodynamic-chemical fluidized bed code. The nature of these source terms for both rapid (e.g., oxidation) and slow (e.g., gasification) reactions is being examined.

A related research area is the examination of particle size distribution upon the fluidized bed flows. In the present code the evolution of particle size is calculated explicitly through numerical accounting procedures which follow the history of the representative Lagrangian particles (c.f. [1]). Thus, as an initially uniform bed of particles experiences nonuniform changes in the particle size, this particle size distribution is "remembered" by the code and the influence of particle size upon the local field properties (e.g., viscosity, drag, etc.) is calculated. An alternative view, which can also account for initially nonuniform particle sizes involves the determination of a particle size distribution and the evolution of this distribution as the flow field develops from its initial state. Some preliminary effort has been initiated on this question; the specific case of particles which do not affect the gas flow can be readily treated. However, the case of coupled gas flow and particle motion requires a simultaneous solution of the field equations [1] and the equation for the evolution of particle size distributions. A discussion of this issue will be presented in the sixth quarterly progress report.

Within the context of the introduction of chemistry into the thermohydrodynamic model we have decided to proceed at first with only those reactions which are most significant (in character and time scale) for the coupling of the chemical reactions and the hydrodynamics. For the case of steam-oxygen gasification this would include, for example, the dominant exothermic reactions in the oxidation of the char and also the water gas shift reaction in the gas phase. Both of these reactions have rapid rates, within the context of time scales associated with the hydrodynamic processes, and in the former case there is significant energy addition to the gas flow. We note that in the first year of this effort [1] we essentially developed chemistry and thermohydrodynamic models separately, with the goal of combining these codes in the second year (c.f. [10]). The chemistry code was a representation of homogeneous reaction in a volumetric element; such a model is appropriate for a reactor which is thoroughly mixed or for a single zone in the finite difference computational model for fluidized beds. This chemistry code is being updated and a parallel quasi-homogeneous reactor model for steam-oxygen gasification is being developed. Both codes will be modularized so that subroutines in these computer models may be directly used in the thermohydrodynamic code (c.f. the following paragraphs). Our present view, as stated above, is that the chemistry will be added to the thermohydrodynamic model in a staged development parallel to the development and improvement of these homogeneous reactor models. This is most necessary in the case of steam-oxygen gasification because of the strong coupling between the chemistry of, say, the oxidation reactions and the transport processes. Thus, when the influence of these strongly coupled processes are established, the additional chemistry associated with the slow rate gasification will be included in the combined chemistry-thermohydrodynamic model.

### Homogeneous Reactor Model/Chemistry Code

The chemistry code representing a time-dependent homogeneous reactor was further modified. This model which includes the chemical reactions appropriate to the $CO_2$ Acceptor process can now be used to represent transient behavior of isothermal, constant volume reactors. Calculations with this code have been performed, to steady state, representing an actual run in the Rapid City Pilot Plant. With gas and solid feed rates appropriate to that run, the calculated exit stream flow rates, exit stream composition and reactor materials inventory are in very good agreement with both direct measurements and estimated data from the pilot plant. This calculation and the related modifications of the homogeneous reactor code are discussed in Appendix B.

There have been some studies, related to chemical parameter optimization, using the modified code. We have found, for example, that the steady state gas composition is affected by, but is not very sensitive to the reaction rate constants for slow rate gasification. In the following quarter we expect to briefly examine the influence of transient inflow and outflow conditions upon the gasification in the $CO_2$ Acceptor process.

The solution of the transient equations in this homogeneous reactor model involves the application of the GEAR[11] method. With this method, a system of first order, ordinary differential equations with many variables can be solved. We expect in the next quarter to extend this model to include non-isothermal reactors; this will require the introduction of another equation for the additional dependent variable: reactor temperature. Within the context of the GEAR method this is conceptually simple; however, there is extensive algebra required in defining rate expressions and matrix elements which are essential to the methodology.

A "homogeneous" reactor model will also be developed for the chemistry of steam-oxygen gasification. This code will likely use the GEAR method of solution for the required transient equations. However, since the oxidation and gasification reactions have rather different time scales, we expect that this "homogeneous" reactor model will be segmented to provide separate descriptions of those respective processes. Further, that chemistry (e.g., aspects of gasification, water-gas shift, devolatilization and prompt methanation) which has been incorporated in the existing homogeneous model for the $CO_2$ Acceptor process, and which can be used in this homogeneous steam-oxygen gasification code, will be so applied. Again, the purpose of this code is to provide a "test bed" for the chemistry and examine methodology which will be incorporated in the thermohydrodynamic computer model with chemistry.

## 3.3 TASK 03 – ENTRAINED FLOW COAL GASIFICATION MODEL

The research on the entrained flow model has included both a review of existing research and the initial formulation of the conservation equations for entrained flows. We plan to develop a field description of the steady* (in a macroscopic time average sense) solid-gas flow in two space dimensions analogous to the continuum representation developed for gas fluidized beds. Of course, since the solid particle loading is much less than that for the emulsion phase of fluidized bed flows, the model for entrained flows will be different in both the inclusion and exclusion of specific physical phenomena. For example, the inertia of the gas is important in entrained flows; this contribution of the gas phase to momentum conservation is neglected in fluidized bed flows. Also the influences of the turbulent nature of the gas phase, in entrained processes, must be represented in the description of momentum conservation.

The nature of our model is best understood within the context of existing models for turbulent flows with chemical

---

*The code will treat transient flow, however our main goal is the calculation of the final steady, or perhaps, stationary flow.

reaction and flows with small particles suspended in them (e.g., dusty gases). There is a growing literature of numerical models for chemically reactive turbulent flows.[12-17] Our model involves a considerable extension of those studies in that the conservation equations for the solid phase together with the appropriate terms for interphase mass, momentum and energy exchange must be included. The solid particles are not merely convected with the gas flow but produce a coupled interaction which can significantly modify the nature of the flow field. There is some analogy between our theoretical model and flow models for dusty gases and fluid droplets.[18-20] However, the nature of the mechanical interactions are different because of the spacing and nature of particles in the present case of entrained flow gasification. Also, in general, it is not possible to assume that the solid particles in entrained flows occupy an insignificant volume. This latter assumption is standard in formulations for dusty gas flows.

In this first quarter a review and summary of theoretical and experimental studies of entrained flows was initiated and it continues. There have been and continue to be theoretical studies of entrained flow gasification. An early, and still useful, model for single stage entrained gasification is that of Batchelder, *et al.*[21] which is based upon the assumption of plug flow in the gasifier. Such representations provide a global behavior of the reactor but offer little insight into the details of the flow field or the residence time in the gasifier. A more recent approach is being examined by Smoot and his coworkers.[22] In that study the flow in the gasifier is assumed to be one-dimensional and steady; the mixing produced by multidimensional turbulence and advection is simulated through the introduction of appropriate coefficients in the equations. Such models together with experimental data can yield important information about the overall process variables. Our approach is rather different in that we are seeking a field description of the flow processes within the gasifier and we thereby calculate, explicitly, such phenomena as multidimensional turbulence and convective mixing in the flow pattern, together with the completely coupled gas-solid particle flow fields. In this context we note the innovative, quasi-one-dimensional model of Harry.[23] He attempts a field description for vortical flow in an entrained flow gasifier. However, this description is based upon several simplifications (e.g., a power series expansion of the field variables in the radial direction, neglect of solid particle dynamics upon the gas flow, the omission of mechanisms related to moderately dense particle clouds, etc.) which make it difficult to assess the resultant calculations.

An interesting article by Dobner[24] ("Modeling of Entrained Bed Gasification: The Issues," EPRI Draft Report, January 15, 1976) summarizes many of the concerns and questions related to entrained flow models for coal gasification. In essence, there is chemistry data for this regime of gasification; however, there is a need, independent of computer modeling, to provide a better definition of the particle heating rates, devolatilization, combustion (including the oxidation of volatiles) and gasification of the particles. We expect to use the existing data and include additional chemistry as it becomes available from current research.

The formulation of the conservation equations for entrained flow was initiated. A description of these equations for flows without turbulence is presented in Appendix C. The turbulent equations, together with some preliminary discussion of turbulent constitutive equations, will be examined in the next quarterly report.

## IV. CONCLUSIONS

In summary we note the following aspects of the modeling effort.

- The chemistry model, in a homogeneous representation of the reactor, provides good agreement with the data from the fluidized bed $CO_2$ Acceptor process. Parametric studies on the influence of the rate constants for the low rate gasification of char suggest that the agreement is somewhat insensitive to these rate constants.

- There is qualitative agreement between the two-dimensional calculations of fluidized bed flows and the two-dimensional measurements of Wen. We expect to perform specific calculations of these experiments in the succeeding months to obtain quantitative comparison with the data.

- The combination of the gasification chemistry with the thermodynamic code for fluidized beds should proceed in a manner where the most dominant reactions (in terms of coupled chemistry and hydrodynamics) are included first. Subsequently, the additional reactions required to specify the complete composition of the outflow of the reactor should be incorporated.

# V. REFERENCES

1. Blake, T. R., S. K. Garg, H. B. Levine and J. W. Pritchett, 1976, Energy Research and Development Administration Report FE-1770-15.

2. Garg, S. K. and J. W. Pritchett, 1975, J. of App. Physics, 46, No. 10, pp. 4493-4500.

3. Jackson, R., 1971, in Fluidization, edited by J. F. Davidson and D. Homison, Academic Press, London and New York.

4. Chapman, S. and T. G. Cowling, 1970, The Mathematical Theory of Non-uniform Gases, 3rd Edition, Cambridge University Press.

5. Murray, J. D., J. Fluid Mechanics, 21, Part 3, pp. 465-493.

6. Schügerl, K., 1971, in Fluidization, edited by J. F. Davidson and D. Homison, Academic Press, London and New York.

7. Walker, P. L., R. Rusinko and L. G. Austin, 1959, Adv. Cataly., XI, pp. 134-221.

8. Mulcahy, M. F. R. and I. W. Smith, 1969, Rev. Pure Appl. Chem., 19, pp. 81-108.

9. Gray, D., J. G. Cogoli and R. H. Essenhigh, 1974, Adv. in Chem., 131, ACS, pp. 72-91.

10. Blake, T. R., 1976, Energy Research and Development Administration Report FE-1770-12.

11. Hindmarsh, A. C., 1974, University of California Report, UCID 3001, Rev. 3.

12. Pantankar, S. V. and D. B. Spalding, 1972, Proc. 14th Intl. Symp. Comb., p. 605.

13. Pantankar, S. V. and D. B. Spalding, 1972, Int. J. Heat and Mass Trans., 15, p. 1787.

14. Gosman, A. D., W. M. Pun, A. K. Runchal, D. B. Spaulding and M. Wolfstein, 1969, Heat and Mass Transfer in Recirculating Flows, Academic Press, New York.

15. Khalil, E. E., D. B. Spaulding and J. H. Whitelaw, 1975, Int. J. Heat and Mass Trans., 18, pp. 775-791.

16. Pantankar, S. V. and D. B. Spaulding, 1974, in Heat Transfer in Flames, Eds. N. Afgan and J. Beer, Scripta, Washington.

17. Gibeling, H. J., H. McDonald and W. R. Briley, 1976, Air Force Aero-Propulsion Laboratory Report 75-59 (Draft).

18. Soo, S. L., 1967, Fluid Dynamics of Multiphase Systems, Blaisdell.

19. Marble, F. E., 1970, in Annual Revies of Fluid Mechanics II, pp. 397-446, Annual Reviews Inc.

20. Edelman, R., M. Rosenbaum and S. Slutsky, 1973, General App. Sci. Lab Technical Report #349.

21. Batchelder, H. R., R. M. Busche and W. P. Armstrong, 1953, I. and E. C., 45, p. 1856.

22. Smoot, L. D. and R. W. Hanks, 1976, Energy Research and Development Administration Report FE-1767-4.

23. Harry, D., 1976, Draft Report, submitted to Foster Wheeler Energy Corporation, Livingston, N. J.

24. Dobner, S., 1976, Draft Report, Electric Power Research Institute, Palo Alto, Ca.

25. Fink, C., G. Curran and J. Sudbury, 1974, "$CO_2$ Acceptor Process Pilot Plant - 1974," Sixth Synthetic Pipeline Gas Symposium, October. Thermal efficiency is defined on page 7 and table IV as the higher heat of combustion of the product gas divided by the higher heat of combustion of feed coal.

26. Curran, G. P., of CDCC, private communication.

27. Coal Conversion Systems Technical Data Book by Institute of Gas Technology for ERDA, February 1976. Page PMa.53.2, Grummel-Davies formula for higher heat of combustion of lignite chars.

28. Anderson, T. B. and R. Jackson, 1967, I&EC Fundamentals, 6, pp. 527-539.

29. Penner, S. S., 1957, Chemistry Problems in Jet Propulsion, Pergammon.

30. Bond, J. W., K. W. Watson and J. A. Welch, 1965, Atomic Theory of Gas Dynamics, Addison Wesley.

31. Blake, T. R. and S. K. Garg, 1976, Water Res. Res., 12, pp. 748-750.

# APPENDIX A

# ON THE BULK VISCOSITY IN MODERATELY DILUTE GAS FLUIDIZATION

## I. INTRODUCTION

In Garg and Pritchett,[2] and Blake, et al.,[1] the governing equations for the motion of gas-fluidized beds, within the framework of continuum theories, are developed. However, the momentum and energy balance relations involve five functions, which must be determined empirically; namely, the normal component of particle-particle interactions $f(\phi)$, where $\phi$ denotes the porosity or voidage, the bulk viscosity of the particle assemblage $\lambda^s(\phi)$, the shear viscosity of the particle assemblage $\mu^s(\phi)$, the local mean drag coefficient $B(\phi)$, and the mixture heat conduction coefficient $\kappa(\phi)$. It is the purpose of this study to give an estimate of the bulk viscosity, since the latter is at present inaccessible to measurement (c.f. Jackson, [3]). The theoretical considerations are based on an assumption of the analogy between moderately dilute particle clouds in gas-solid flows and dense gases in the treatise of Chapman and Cowling.[4] In what follows, their results will be adopted accordingly. Within this context, we note that the momentum exchange associated with solid particle motion in gas-fluidized beds can be associated with two major mechanisms of transport. First there is the particle-particle interaction which results from collisions between particles. This interaction involves both normal and tangential collisions. The former lead, on a continuum basis, to hydrostatic forces, while the latter contribute to shearing forces in fluidized beds. Second, and to a lesser extent, there is the momentum exchange associated with particle transport on a random basis. In the case of dense particle packing it is expected that the particle-particle interactions dominate and that both normal and tangential collisions must be accounted for. For the case of moderate to very dilute particle distributions, we expect that normal collisions and random particle motions dominate the momentum exchange. In that latter regime there is a direct analogy between the assemblage of solid particles and a dense gas. We use that analogy to investigate the relationship between bulk and shear viscosities for the solid particle assemblage. This solid particle assemblage, or cloud, in the dilute regime is not of major interest to gas fluidized beds. However, we expect that our conclusions with respect to the relative orders of magnitudes of bulk and shear viscosities asymptotically apply to the dense particle clouds which comprise the bulk of the emulsion phase in such beds.

## II. ANALYSIS

Consider a particle cloud composed of non-porous rigid spherical masses of diameter $\sigma$. Denoting the number density of the particles, i.e., the number of particles per unit volume, by n, and the mass of any particle by m, the (true) mass-density $\rho_p^s$ of the particle cloud or assemblage at a given instant of time and position of the center of the particle can be written in the form

$$\rho_p^s = nm \qquad (A.1)$$

with

$$b\rho_p^s = \frac{2}{3} n\pi\sigma^3 \qquad (A.2a)$$

$$b = \frac{2}{3} \frac{\pi\sigma^3}{m} \qquad (A.2b)$$

From analogy with the case of dense gases (Chapman and Cowling)[4] we obtain for the shear viscosity coefficient of this moderately dilute particle assemblage

$$\mu^s = \mu_0^s \, \chi^{-1}\left(1 + \frac{2}{5}\, b\, \rho_p^s \, \chi\right)^2 + \frac{3}{5}\lambda^s \tag{A.3}$$

where $\mu_0^s$ denotes the viscosity of a very dilute cloud of particles. In terms of $\mu_0^s$, the bulk viscosity is given by

$$\lambda^s = 1.002\, \mu_0^s \, \chi \, (b\rho_p^s)^2 \tag{A.4}$$

while the value of $\chi$ is found to be

$$\chi = 1 + \frac{5}{8}\,(b\rho_p^s) + 0.2869(b\rho_p^s)^2 + 0.1103(b\rho_p^s)^3$$
$$+ 0.0386(b\rho_p^s)^4 + \ldots \tag{A.5}$$

The quantity $\chi$ is equal to unity for a very dilute particle assemblage and increases with increasing density. If the assemblage approaches the state in which the particles are packed so closely that motion is impossible, $\chi$ tends to infinity. Within this context, the asymptotic behavior of viscosity of this moderately dilute particle cloud is consistent with that of a tightly packed bed of particles.[1]

Denoting the solidity (solid volume fraction = 1 - voidage) by $\theta$, the (superficial) density of the solid reads

$$\rho^s = \theta\rho_p^s = (1-\phi)\,\rho_p^s \tag{A.6}$$

Furthermore,

$$\theta = 1 - \phi = n\tau \tag{A.7}$$

where $\tau$ is the volume of an individual particle. Since the particles are assumed to be spherical ($\tau = \pi\sigma^3/6$), Eqs. (A.2) and (A.7) yield

$$b\rho_p^s = 4(1-\phi) \tag{A.8}$$

Therefore, we can calculate $\chi$ as a function of solidity $(1-\phi)$, namely

$$\chi(\theta) = \chi(1-\phi) = 1 + 2.5(1-\phi) + 4.5904(1-\phi)^2 + 7.0592(1-\phi)^3 + 9.8816(1-\phi)^4 + \ldots \quad (A.9)$$

Eliminating $\mu_0^s$ in (A.3) by means of (A.2) leads to

$$\frac{\mu^s}{\lambda^s} = 0.6 + \frac{1}{16.032(1-\phi)} \quad \frac{[1 + 1.6(1-\phi)\chi]^2}{\chi^2} \quad (A.10)$$

The limiting cases $\chi \to 1$ and $\chi \to \infty$ deserve special mentioning:

a, <u>$\chi \to 1$ $(\phi \to 1)$</u>. It follows immediately that the bulk viscosity approaches zero; hence, according to Eq. (A.3), $\mu^s \to \mu_0^s$.

b. <u>$\chi \to \infty$ $(\phi \to 0.4)$</u>. Straightforward manipulation of Eq. (A.10) reveals that $\mu^s \approx 0.76\ \lambda^s$. This demonstrates clearly that $\mu^s$ and $\lambda^s$ are of the same order of magnitude; however $\lambda^s > \mu^s$.[5]

In order to complete the evaluation of the bulk viscosity, the shear viscosity must be known explicitly. In the case under consideration, let us assume, for the sake of illustration, that $\mu^s$ behaves like the shear viscosity of rather dense particle clouds associated with moderate bed expansions. We introduce $(1-\phi)/(\phi-\phi_0)$, where $\phi_0$ denotes the minimum bed porosity of a fluidized bed. Following [1], we define

$$\bar{\mu}^s = \frac{2.65\ \mu^s}{100\ \rho^s d^2} \quad (A.11)$$

where $d(= 2\sigma)$ is the particle diameter. A correlation of the experimental data reported by Schügerl[6] leads to

$$\bar{\mu}^s = 4.35 + 0.13\,\frac{1-\phi}{\phi-\phi_0}\ ,\quad 2 \le \frac{1-\phi}{\phi-\phi_0} \leqq 25 \tag{A.12}$$

Finally, employing Eqs. (A.11) and (A.12), we obtain

$$\lambda^s = \frac{100\,\rho^s d^2}{2.65}\left(4.35 + 0.13\,\frac{1-\phi}{\phi-\phi_0}\right)\left\{0.6 + \frac{[1+1.6(1-\phi)\chi]^2}{16.032(1-\phi)^2\chi^2}\right\}^{-1} \tag{A.13}$$

Thus we obtain an expression for $\lambda^s$ based upon theoretical considerations for a moderately dilute cloud of particles together with an empirical measurement of $\mu^s$. Of course, we have extrapolated our theory to the regime of very dense particle clouds in order to use existing data. However, the main point is that the theory provides us with a relationship for $\lambda^s$ in terms of $\mu^s$, (c.f. (A.10) and the associated discussion) which asymptotically defines the relative order of magnitude of these viscosities in the limit of very dense solid particle clouds.

# APPENDIX B

## STATUS OF THE $CO_2$ ACCEPTOR MODEL

Since our annual report of July 1976,[1] the $CO_2$ acceptor model has undergone changes which enable it to more nearly duplicate actual gasifier processes, so that the code in its representation of a homogeneous reactor is quite general. In particular, the code can now treat variable pressure for a constant volume reactor. Further, we have expanded the output information, and the code has been restructured.

Conversion to variable pressure involved a very straightforward use of the ideal gas law

$$P = \frac{nRT}{V - \sum_i n_i v_i} \qquad i = \text{condensed phases} \tag{B.1}$$

where $n$ represents total moles of gas and $v_i$ is the molar volume of a solid. Since gas partial pressures are now available, it is reasonable to set gas exit rates proportional to their partial pressures

$$N_i = a \frac{n_i}{n} (P - P_s) \tag{B.2}$$

$P_s$ represents sink back pressure and $a$ is a proportionality factor calculated from experimental conditions.

Concurrently with the variable pressure code development, three new chemical constituents were introduced. These arise from division of char into fixed carbon and ash components, and from division of acceptor into active CaO, $CaCO_3$, and inerts. As a result, kinetics involving these components can now be treated accurately by the GEAR package.

Variable temperature has been subsequently added. It will be reviewed in our next quarterly report. Essentially, temperature was treated as an additional time-dependent variable to be integrated by the GEAR package along with mole numbers of chemical constituents.

Additional outputs from the code include a more sophisticated plot package using a pen plotter, a feature for introduction of transients, a checkpoint-restart feature, and a thermal efficiency evaluation as defined by Fink, *et al.*[25] The thermal efficiency may be used as a basis for comparison in calculations to optimize the reactor.

The numerical integration of rate equations was found to run faster in double precision, presumably due to increased accuracy in the predictor-corrector cycle. Therefore, the GEAR package integration scheme has been converted to run entirely in double precision, including the matrix inversion step. Computer time required to reach steady state from startup is 5.7 seconds on the Univac 1108. The corresponding reactor time is 2026 minutes.

## CALCULATION OF THE $CO_2$ ACCEPTOR PROCESS

A calculation, to steady state, of the $CO_2$ acceptor process was performed with the modified code. For the most part, inputs to the new version of the $CO_2$ acceptor model are the same as those described in [1]. However, some changes, as indicated in Table B.1, were required. Some of these changes were necessary to implement the variable pressure feature, while others provide improved estimates for the variables concerned. The input parameters relating to boundary and initial conditions for the test calculations are shown in Tables B.2 and B.3. With these conditions, the initial value problem of reactor startup and evolution to steady state was calculated.

## TABLE B.1

## CHANGES IN INPUTS TO THE $CO_2$ ACCEPTOR CODE

| Variable | Previous Value | Present Value |
|---|---|---|
| Reactor Pressure, P | 9.3 atm | 8.9[c] |
| Reactor Volume, V | 12340[c] liters | 13097 liters |
| Gas Exit Parameter, a | Redefined | 240.9 moles $atm^{-1}$ $min^{-1}$ |
| Gas Exit Parameter, $a_1$ | 1.732 moles/min | Discontinued |
| Ash Steady State Inventory, $U_{ash}$ | -- | $3.021 \times 10^5$ g |
| Inert Steady State Inventory, $U_{inert}$ | -- | $1.3956 \times 10^6$ g |
| Char Exit Rate Parameter, $a_8$ | $4.502 \times 10^{-3}$ $min^{-1}$ | Discontinued |
| Acceptor Exit Rate Parameter, $a_9$ | $3.369 \times 10^{-3}$ $min^{-1}$ | Discontinued |
| Ash Catalysis Factor, $\theta$ | 0.005 | 0.0001 but irrelevant |
| Char Heat of Combustion | 6659[e] cal/g HHV | 7177 cal/g HHV[22] |
| Mean Acceptor Particle Diameter, $\phi$ | -- | 0.1562 cm |

[c] Computed rather than input value

[e] Rough estimate

## TABLE B.2

## INPUT PARAMETERS FOR A TEST OF THE COAL2B PROGRAM AGAINST EXPERIMENT

| | |
|---|---|
| Lignite Heat of Combustion | 6310 cal/g (measured HHV at 60°F) |
| Char Heat of Combustion | 7177 cal/g[22] (estimated HHV at 60°F) |
| Lignite Feed Rate to Gasifier, r | 18522 g/min |
| Steam Feed Rate Ratio, 2 | 1.07 g/g lignite |
| Acceptor Feed Rate Ratio, a | 3.59 g/g lignite |
| Steam Feed Temperature | 1066°K |
| Acceptor Feed Temperature | 1278°K |
| Lignite Feed Temperature | 478°K |
| Reactor Operating Temperature, T | 1085°K |
| Reactor Volume, V | 13100 liters |
| Ash Catalytic Activity Factor, $\Theta$ | 0.005 |
| Acceptor Activity Factor, $\Theta_a$ | 0.37 |
| Initial CaO Reacted Fraction, $\rho_0$ | 0.99 |
| Gas Exit Rate Parameter, $a_1$ | 241 moles/(atm min) |
| Gas Exit Back Pressure, $P_s$ | 1.0 atm |
| Recycle Ratio, $\Theta_c$ | 0.2323 |
| Ash Steady State Inventory | $3.021 \times 10^5$ g |
| Inerts Steady State Inventory | $1.3956 \times 10^6$ g |

## TABLE B.3

## STARTUP CONDITIONS FOR A TEST RUN OF THE COMPUTER PROGRAM

| | |
|---|---|
| Reactor Inventory | |
| $H_2$, $CH_4$, $CO$, $CO_2$, $N_2$, $H_2S$ | 1.0 moles |
| $H_2O$ | 1116 moles |
| Char | $1.361 \times 10^6$ grams |
| Acceptor (active fraction 99 percent carbonated) | $1.957 \times 10^6$ grams |

Reactor pressure, gas phase concentrations, and some other interesting time-dependent variables are illustrated in Figures B.1 - B.6. These figures illustrate reaction progress during the first sixty minutes following reactor startup. They are subject to two caveats: Since the calculation is isothermal, temperature-dependent effects are neglected. Second, because the code contains no oxidation mechanism, the initial heat duly provided by combustion cannot be treated.

Except for changes in mean acceptor and char composition, which are gradual because of the large amount of material involved, the gasifier reaches steady state in the sixty minute period shown. The reactor pressure begins near its steady state value, rises to a peak of 10.6 atm in less than a minute, and subsides to 8.9 atm at steady state. Experimental steady state reactor pressure is 9.3 atm absolute.

Other outputs from the current version of the $CO_2$ acceptor code, designated COAL2B, are shown in Tables B.4 - B.8. They are displayed in comparison with experimental results from the Rapid City pilot plant.[26] No great differences exist between these and the results reported in [1]. On a mole percent basis, calculated exit gas is richer in $CH_4$ and poorer in $H_2$ and $H_2O$ than previously calculated. Thermal efficiency is 72.2 percent, in good agreement with the value of 77 percent reported in [25]. When the more realistic nonisothermal version of the code is reported, we may anticipate still better agreement with experiment.

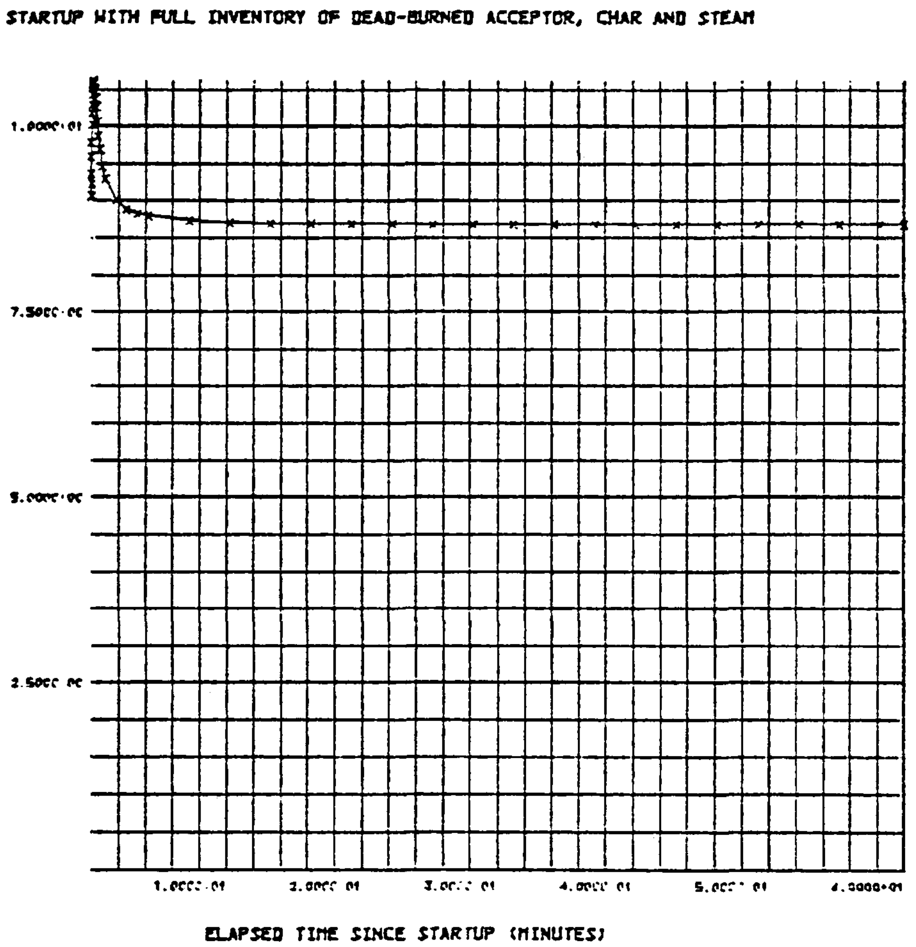
STARTUP WITH FULL INVENTORY OF DEAD-BURNED ACCEPTOR, CHAR AND STEAM
REACTOR PRESSURE (ATMOSPHERES)
1.0000+01
7.5000+00
5.0000+00
2.5000+00
1.0000+01
2.0000+01
3.0000+01
4.0000+01
5.0000+01
6.0000+01
ELAPSED TIME SINCE STARTUP (MINUTES)

Figure B.1

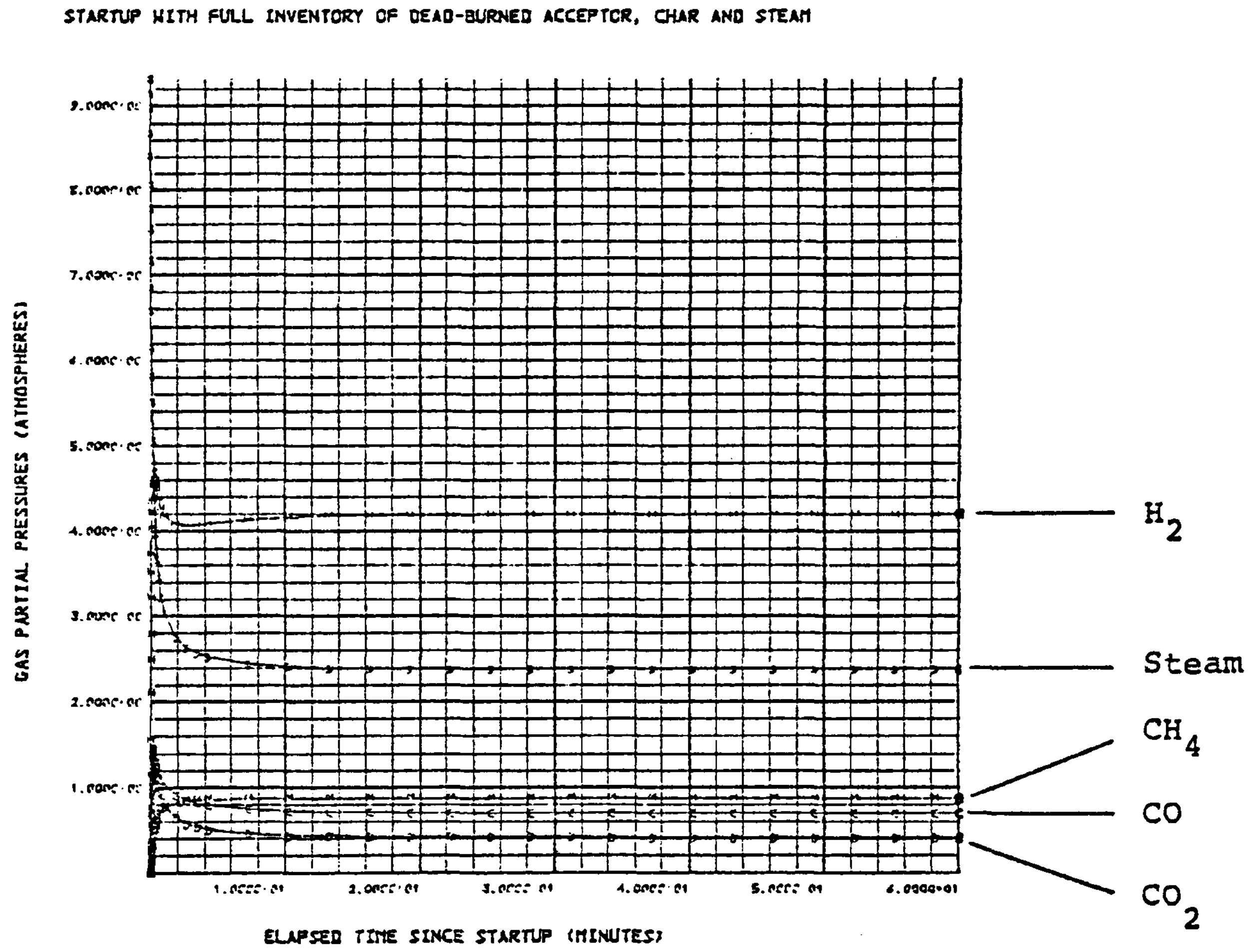
STARTUP WITH FULL INVENTORY OF DEAD-BURNED ACCEPTOR, CHAR AND STEAM
GAS PARTIAL PRESSURES (ATMOSPHERES)
9.0000E+00
8.0000E+00
7.0000E+00
6.0000E+00
5.0000E+00
4.0000E+00
3.0000E+00
2.0000E+00
1.0000E+00
1.0000E+01
2.0000E+01
3.0000E+01
4.0000E+01
5.0000E+01
6.0000E+01
ELAPSED TIME SINCE STARTUP (MINUTES)
$H_2$
Steam
$CH_4$
CO
$CO_2$

Figure B.2

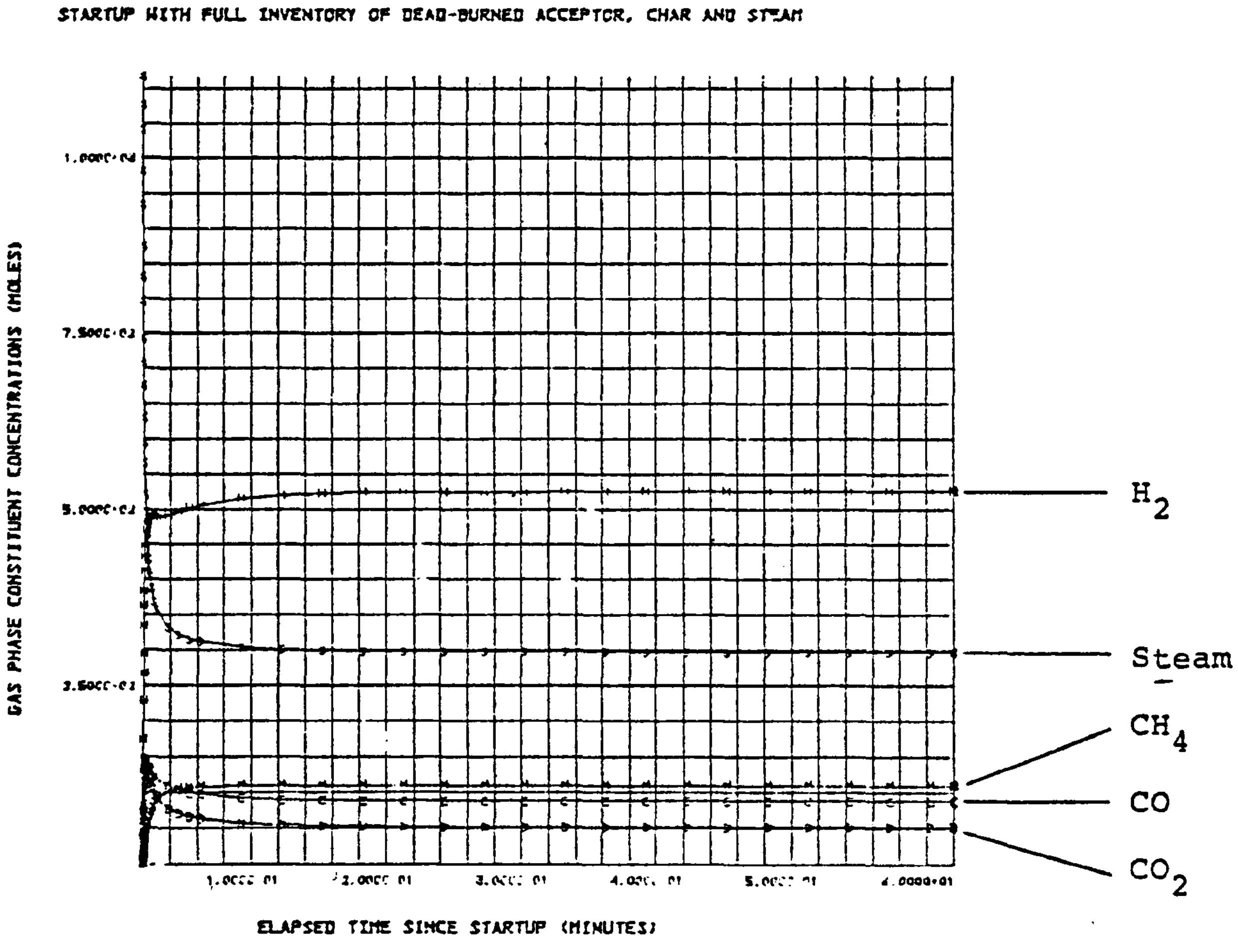
STARTUP WITH FULL INVENTORY OF DEAD-BURNED ACCEPTOR, CHAR AND STEAM
GAS PHASE CONSTITUENT CONCENTRATIONS (MOLES)
1.0000+03
7.5000+02
5.0000+02
2.5000+02
1.0000+01
2.0000+01
3.0000+01
4.0000+01
5.0000+01
6.0000+01
ELAPSED TIME SINCE STARTUP (MINUTES)
$H_2$
Steam
$CH_4$
CO
$CO_2$

Figure B.3

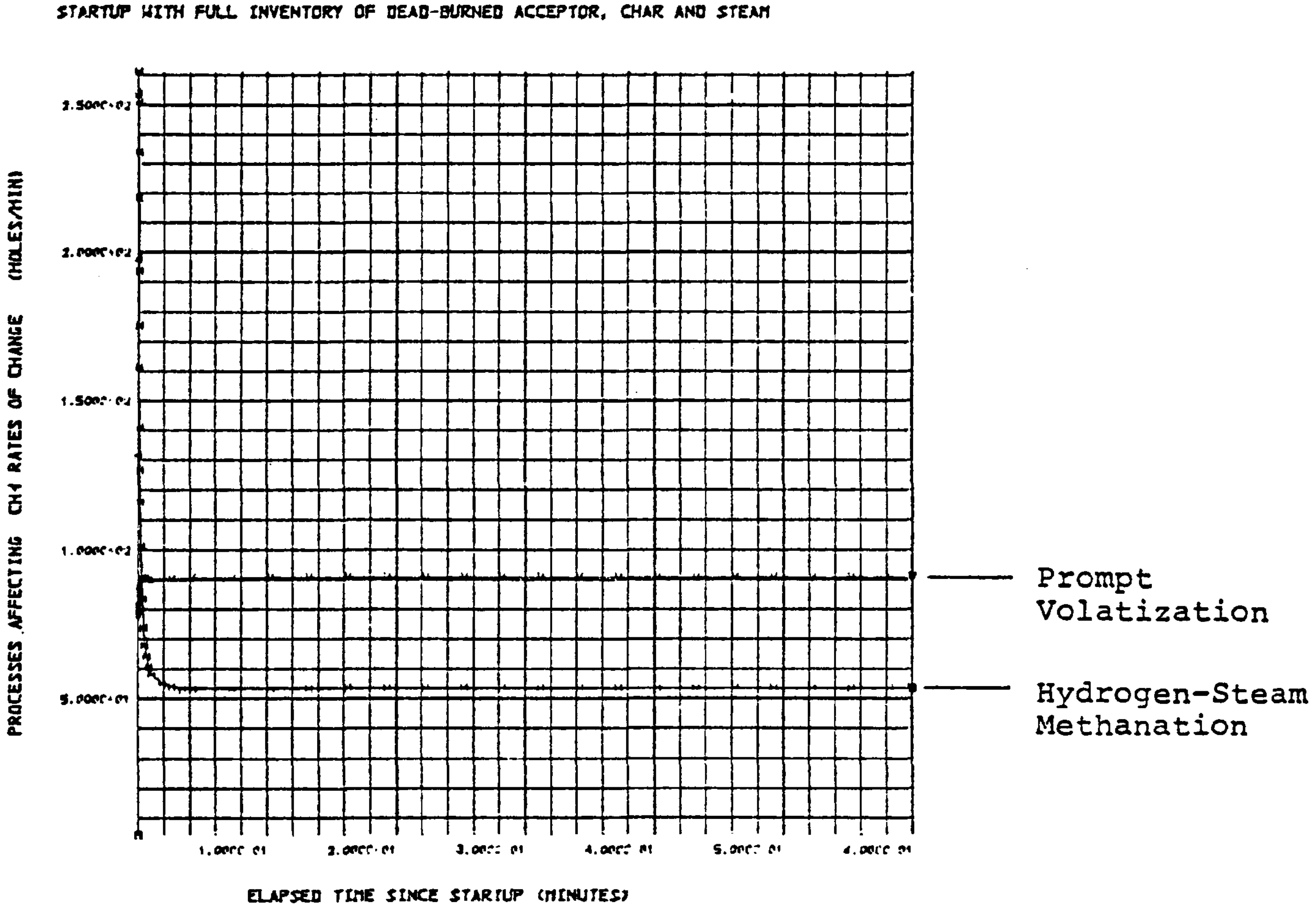
STARTUP WITH FULL INVENTORY OF DEAD-BURNED ACCEPTOR, CHAR AND STEAM
PROCESSES AFFECTING CH4 RATES OF CHANGE (MOLES/MIN)
2.5000E+02
2.0000E+02
1.5000E+02
1.0000E+02
5.0000E+01
0
1.0000E 01
2.0000E+01
3.0000E 01
4.0000E 01
5.0000E 01
6.0000E 01
ELAPSED TIME SINCE STARTUP (MINUTES)
Prompt Volatization
Hydrogen-Steam Methanation

Figure B.4

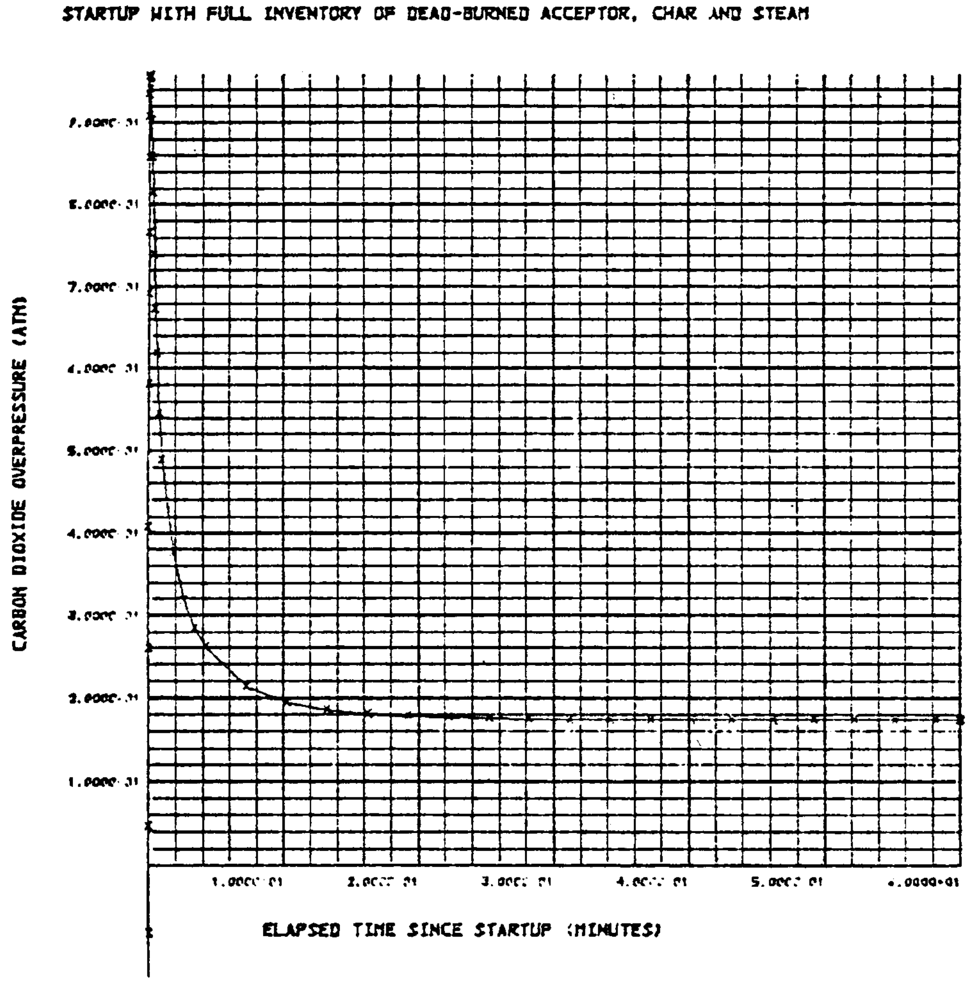
STARTUP WITH FULL INVENTORY OF DEAD-BURNED ACCEPTOR, CHAR AND STEAM
CARBON DIOXIDE OVERPRESSURE (ATM)
9.0000-01
8.0000-01
7.0000-01
6.0000-01
5.0000-01
4.0000-01
3.0000-01
2.0000-01
1.0000-01
1.0000+01
2.0000+01
3.0000+01
4.0000+01
5.0000+01
6.0000+01
ELAPSED TIME SINCE STARTUP (MINUTES)

Figure B.5

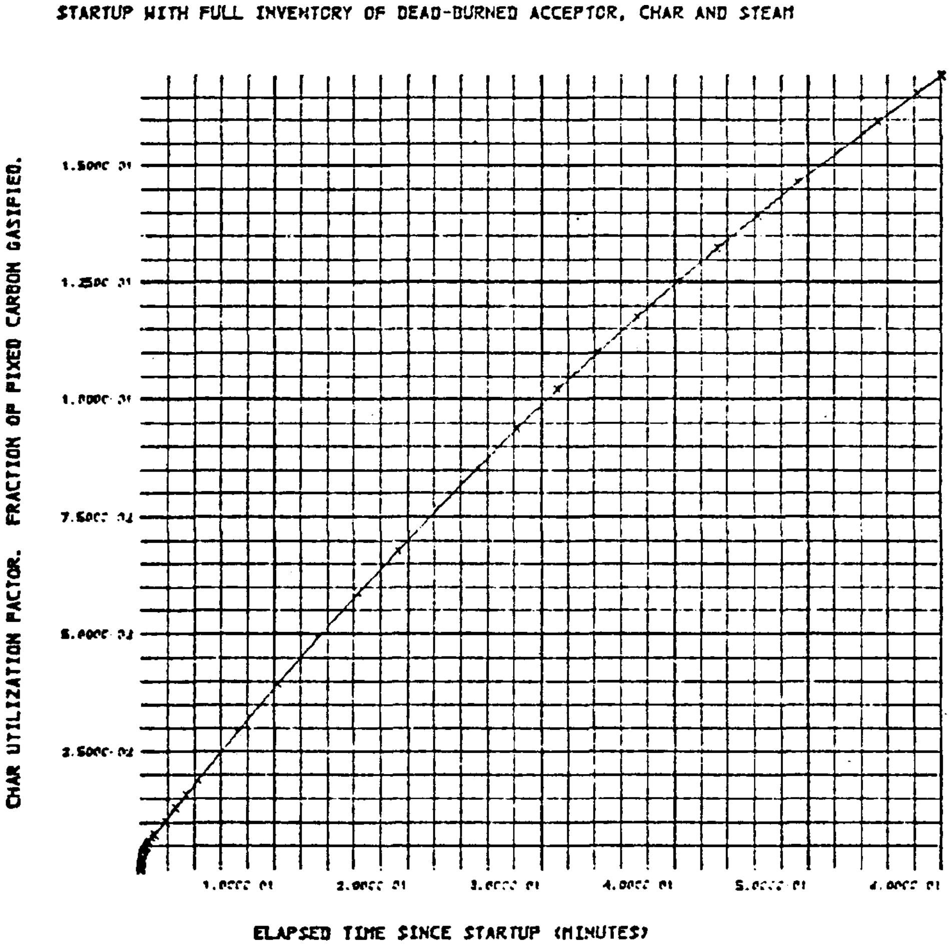
STARTUP WITH FULL INVENTORY OF DEAD-BURNED ACCEPTOR, CHAR AND STEAM
CHAR UTILIZATION FACTOR. FRACTION OF FIXED CARBON GASIFIED.
1.500E-01
1.250E-01
1.000E-01
7.500E-02
5.000E-02
2.500E-02
1.000E 01
2.000E 01
3.000E 01
4.000E 01
5.000E 01
6.000E 01
ELAPSED TIME SINCE STARTUP (MINUTES)

Figure B.6

## TABLE B.4

## MATERIALS INVENTORIES IN THE REACTOR IN STEADY STATE OPERATION

| Material (Units) | Computed | Estimated, Pilot Plant |
|---|---|---|
| Hydrogen (moles) | 446 | 490 |
| Steam (moles) | 301 | 286 |
| Methane (moles) | 99 | 113 |
| Carbon Monoxide (moles) | 101 | 127 |
| Carbon Dioxide (moles) | 72 | 75 |
| Nitrogen (moles) | 4 | 26 |
| Hydrogen Sulfide (moles) | 2 | 1 |
| Ammonia (moles) | 0 | 6 |
| Acceptor (grams)* | $1.95 \times 10^6$ | $1.96 \times 10^6$ |
| Char (grams) | $1.51 \times 10^6$ | $1.36 \times 10^6$ |

---

*Total mass, including absorbed $CO_2$

## TABLE B.5

## COMPUTED AND OBSERVED THERMODYNAMIC RATIOS IN STEADY STATE OPERATION

| Reaction | Ratio | Computed | Observed, Pilot Plant |
|---|---|---|---|
| Water Gas Shift | $Q_W$ | 1.00 | 0.96 |
| Methane Steam Reforming | $Q_H$ | 10.19 | 7.28 |
| Methane Cracking | $Q_G$ | 1.48 | 1.45 |

## TABLE B.6

## COMPUTED AND OBSERVED EXIT STREAM FLOW RATES AT STEADY STATE

| Material (Units) | Computed | Observed, Pilot Plant |
|---|---|---|
| Char (g/min) | 6351 | 6123 |
| Acceptor (g/min)* | 75860 | 76100 |
| Unreacted Steam (g/min) | 10170 | 9223 |
| Product Gas (dry basis) (g/min) | 12450 | 14290 |

---

*Includes absorbed $CO_2$

# TABLE B.7

# COMPUTED AND OBSERVED COMPOSITION OF ACCEPTOR AND CHAR EXIT STREAMS OF THE $CO_2$ ACCEPTOR PILOT PLANT OPERATING AT STEADY STATE

| Acceptor | Computed | Observed, Pilot Plant |
|---|---|---|
| CaO (weight percent) | 43.6 | 43.5 |
| MgO (weight percent) | 36.1 | 36.0 |
| Inert (weight percent) | 7.9 | 7.9 |
| $CO_2$ (weight percent) | 12.4 | 12.6 |

| Char | Computed | Observed,* Pilot Plant |
|---|---|---|
| C (weight percent) | 78.8 | 76.5 |
| H (weight percent) | 0.9 | 0.9 |
| O (weight percent) | 0.0 | 0.0 |
| N (weight percent) | 0.4 | 0.4 |
| S (weight percent) | 0.0 | 0.0 |
| Ash (weight percent) | 20.0 | 22.2 |

---

*Weighted average of char stream to regenerator and char fines lost via cyclone

## TABLE B.8

## PRODUCT GAS COMPOSITION (DRY BASIS) OF THE $CO_2$ ACCEPTOR PILOT PLANT OPERATING AT STEADY STATE

| Component (Units) | Computed | Observed, Pilot Plant |
|---|---|---|
| $H_2$ (mole percent) | 61.6 | 59.0 |
| $CH_4$ (mole percent) | 13.7 | 13.5 |
| CO (mole percent) | 14.0 | 15.2 |
| $CO_2$ (mole percent) | 9.9 | 9.0 |
| $N_2$ (mole percent) | 0.55 | 3.2 |
| $H_2S$ (mole percent) | 0.3 | 0.1 |
| $NH_3$ (mole percent) | - | 0.5 |

# APPENDIX C

## CONSERVATION EQUATIONS FOR ENTRAINED FLOWS WITHOUT TURBULENCE

In this appendix we summarize the derivation of continuum equations for entrained flows, based upon the method of Anderson and Jackson.[28]

### MATHEMATICAL PRELIMINARIES

In the Anderson and Jackson methodology, a formal technique, incorporating the concept of a weighting function, is used to replace point variables by local mean variables. Specifically if $\psi'$ is a point variable in the fluid phase of the flow, then a local mean variable $\psi$ is defined by:

$$\psi(x_i,t) \int_f g\,(|x_i - y_i|)\, dV\,(y_i)$$

$$= \int_f \psi'\,(y_i,t)\, g\,(|x_i - y_i|)\, dV\,(y_i) \qquad \text{(C.1)}$$

where $g\,(|x_i - y_i|) = g(r)$ is the weighting function and where the integrals are taken over the volume occupied by the fluid phase at time t. (In these integrals, the use of repeated subscripts in the arguments of the indicated functions does not imply summation. This notation will be used throughout; tensorial summation will only apply when repeated subscripts appear on the function itself.)

The weighting function has the properties

$$r > 0: \quad g(r) \geq 0, \; \frac{dg(r)}{dr} \leq 0$$

and

$$4\pi \int_0^\infty g(r)\, r^2 dr = 1$$

Further, we require that g(r) possess derivatives of all orders and that the corresponding volume integrals of these derivatives exist. The radius, R, of the weighting function is defined as

$$4\pi \int_0^R g(r)\, r^2 dr = \frac{1}{2}$$

If $\ell$ is a characteristic local dimension of the solid particles and $L$ is a characteristic dimension of the complete fluid-solid system, it is assumed that

$$\ell << R << L$$

With this restriction, the actual structure of the weighting function is unimportant; the relationship between the local mean porosity $\phi$ and the weighting function, satisfying the above restrictions can now be stated. This is expressed as

$$\phi(x_i,t) = 1 - \theta(x_i,t) = \int_f g\,(|x_i - y_i|)\; dV\;(y_i) \qquad \text{(C.2)}$$

Further, the spatial variation of the local mean variable is small compared with that of the weighting function and we have, with (C.2) that

$$\int_f \psi(y_i,t)\; g\;(|x_i-y_i|)\; dV\;(y_i) \simeq \psi(x_i,t)\phi(x_i,t) \qquad (C.3)$$

The point variable $\psi'$ is expressed as the sum of the local mean variable $\psi$ and a fluctuation about that mean value $\psi''$, namely

$$\psi'(x_i,t) = \psi(x_i,t) + \psi''(x_i,t) \qquad (C.4)$$

where $\psi''$ reflects behavior on a length scale appropriate to the particle. In this context, turbulence on a scale large compared to the particle radius can be naturally included in the terms $\psi'$ and $\psi$. With (C.3) and (C.4) it follows that the local mean value of the fluctuation is much smaller than (C.3), and it can be neglected; that is

$$\int_f \psi''(y_i,t)\; g\;(|x_i-y_i|)\; dV\;(y_i) << \int_f \psi(y_i,t)\; g\;(|x_i-y_i|)\; dV\;(y_i) \simeq \psi(x_i,t)\phi(x_i,t) \qquad (C.5)$$

This inequality will permit significant simplifications in the derivation of the conservation equations for the local mean variables. In addition, we will need relationships between the temporal and spatial derivatives of the local mean variables and those respective derivatives of the point variables. These relationships are derived by Anderson and Jackson and are given by

$$\int_f \frac{\partial\psi'}{\partial t}\;(y_i,t)g(|x_i-y_i|)\;dV(y_i) = \frac{\partial}{\partial t}\;\phi(x_i,t)\psi(x_i,t)$$

$$+\int \psi'(y_i,t)\;n_k v_k^b\;(y_i,t)g(|x_i-y_i|)\;dA(y_i) \qquad (C.6a)$$

$$\int_f \frac{\partial\psi'}{\partial y_j}(y_i,t)g(|x_i-y_i|)\,dV(y_i) = \frac{\partial}{\partial X_j}\,\phi(x_i,t)\psi(x_i,t)$$

$$-\int\psi'(y_i,t)n_j g(|x_i-y_i|)\,dA(y_i) \qquad \text{(C.6b)}$$

where the integrals on the right hand side of (C.6) are taken over the fluid-solid interface which is a surface bounding the fluid phase and $n_j$ is a unit normal vector directed into the fluid volume; $v_k^b$ is the local velocity of this bounding surface. Since the solid phase is composed of discrete particles, we may write the surface integrals as a summation over the particles, P

$$\int\psi'(y_i,t)n_j g(|x_i-y_i|)dA(y_i) = \sum_P \int_P \psi'(y_i,t)g(|x_i-y_i|)n_j\, dA_P(y_i) \qquad \text{(C.7)}$$

## CONSERVATION EQUATIONS FOR LOCAL MEAN VARIABLES

We assume that at a point, $y_i$, in the gas phase, the principles of conservation of mass, momentum and energy can be described by the following differential equations: where tensorial notation is used,

$$\frac{\partial\rho'_\alpha}{\partial t} + \frac{\partial\rho'_\alpha v'_i}{\partial y_i} = \Omega'_\alpha \qquad \text{(C.8)}$$

$$\frac{\partial\rho' v'_i}{\partial t} + \frac{\partial}{\partial y_j}\rho' v'_i v'_j = \frac{\partial\sigma'_{ij}}{\partial y_j} + \rho' g_i \qquad \text{(C.9)}$$

$$\frac{\partial}{\partial t}\rho'\left(e' + \frac{v'_i v'_i}{2}\right) + \frac{\partial}{\partial y_j}\rho' v'_j\left(e' + \frac{v'_i v'_i}{2}\right)$$

$$= \frac{\partial}{\partial y_j} v'_i\sigma'_{ij} + \rho' g_i v'_i - \frac{\partial q'_i}{\partial y_i} \qquad \text{(C.10)}$$

We write a conservation of mass equation for each species with density $\rho'_\alpha$, where the summation of these equations over the species yields a conservation equation for the gas with the density of the gas given by $\rho' = \sum_\alpha \rho'_\alpha$; the diffusion of species $\alpha$ is neglected. The remaining point variables $v'_i$, $e'$, $\sigma'_{ij}$, $q'_i$ are respectively the gas velocity, specific internal energy, stress tensor and heat flux vector. We note that both $e'$ and $q'_i$ may include diffusion contributions (c.f., Penner[29] and Bond, _et al._[30]) and that radiative transport may be included in $q'_i$. The specific internal energy $e'$ implicitly contains the heat of formation and consequently evolution of heat from chemical reaction is included in the transport of this quantity. The corresponding equations for the local mean variables are obtained by a spatial average of (C.8)-(C.10). We, therefore, multiply those equations by the weighting function $g(|x_i-y_i|)$ and integrate over the fluid volume. With (C.1), (C.2), (C.4), (C.6) and (C.7), we obtain for the conservation of mass and momentum*

$$\frac{\partial}{\partial t} \phi \rho_\alpha + \frac{\partial}{\partial x_i} \phi \rho_\alpha v_i + \frac{\partial R_{\alpha i}}{\partial x_i} = S_\alpha + \phi \Omega_\alpha \qquad (C.11)$$

$$\frac{\partial}{\partial t} \phi \rho v_i + \frac{\partial}{\partial x_j} \phi \rho v_i v_j + \frac{\partial R_i}{\partial t} = \frac{\partial}{\partial x_j} (\sigma_{ij} - R_{ij})$$

$$+ M_i + \phi \rho g_i \qquad (C.12)$$

In these equations, the integrals representing fluctuations are

---

*In this presentation for simplicity we will implicitly assume that the particle volume decreases with mass loss. We note that the species transport equation has been examined by Blake and Garg.[31]

$$R_{\alpha i} = \int_f \rho_\alpha'' v_i'' \; g|x_k-y_k| dV, \quad R_i = \sum_\alpha R_{\alpha i}$$

$$R_{ij} = \int_f \left\{ \rho v_i'' v_j'' + \rho'' v_i'' v_j + \rho'' v_i v_j'' + \rho'' v_i'' v_j'' \right\}$$

$$\cdot \; g|x_k-y_k| dV$$

and the interphase mass and momentum exchange are represented respectively by

$$S_\alpha = - \sum_P \int_P \rho_\alpha' \left( v_k^b - v_k' \right) n_k \; g|x_i-y_i| dA_P, \quad S = \sum S_\alpha$$

$$M_i = - \sum_P \int_P \left\{ \rho' v_i' \left( v_k^b - v_k' \right) + \sigma_{ik}' \right\} n_k \; g|x_i-y_i| dA_P$$

In these expression S and $M_i$ must be further defined in terms of the average flow properties to provide closure. We will examine such closure in a subsequent paragraph.

The conservation of energy for the gas phase is

$$\frac{\partial}{\partial t} \left[ \rho\phi \left( e + \frac{v_i v_i}{2} \right) \right] + \frac{\partial}{\partial X_j} \left[ \rho\phi \; v_j \left( e + \frac{v_i v_i}{2} \right) \right]$$

$$+ \frac{\partial}{\partial t} \left\{ E + \frac{1}{2} R_{kk} \right\} + \frac{\partial E_j}{\partial X_j}$$

$$= \frac{\partial}{\partial X_j} v_i (\sigma_{ij} - R_{ij}) - \frac{\partial \phi q_i}{\partial X_j}$$

$$+ N + \phi \; \rho \; v_i g_i + g_i R_i \qquad \text{(C.13)}$$

where again the influence of fluctuations is contained in the integral $R_{ij}$ and in the following

$$E = \int_f \rho'' e'' \; g|x_k - y_k| dV$$

$$\begin{aligned} E_j = \int_f \Big\{ & \rho v_j'' e'' + \rho'' v_j e'' + \rho'' v_j'' e + \rho'' v_j'' e'' \\ & + \frac{1}{2} \Big[ \rho'' v_j'' \left( v_i'' v_i'' - v_i v_i \right) + \rho v_j v_i'' v_i'' \\ & + \rho v_i'' v_i'' v_i'' \Big] - v_i'' \sigma_{ij}'' \Big\} \; g|x_k - y_k| dV \end{aligned}$$

The interphase energy exchange is represented by the integral

$$\begin{aligned} N \equiv - \sum_P \int_P \Big\{ & \rho' \left( v_k^b - v_k' \right) \left( e' + \frac{v_i' v_i'}{2} \right) \\ & + v_i' \sigma_{ik}' - q_k' \Big\} \; n_k \; g|x_i - y_i| dA_P \end{aligned}$$

The equations for a single particle with the assumptions of constant density, rigidity, uniform composition and uniform intraparticle velocity and temperature fields, are

$$\rho^s \frac{d\upsilon'}{dt} = \rho^s \int_P \left( v_i^b - u_i' \right) n_i \; dA_P \qquad \text{(C.14)}$$

$$\begin{aligned} \rho^s \frac{d}{dt} \left( \upsilon' u_i' \right) = & \int_P \sigma_{ij}' n_j dA_P + \rho^s \upsilon' g_i \\ & + \int_P \rho^s u_i \left( v_i^b - u_i' \right) n_i dA_P \end{aligned} \qquad \text{(C.15)}$$

for the conservation of mass and momentum, respectively. In these equations, $\int_p \sigma_{ij}' n_i dA_P$ represents the force of the gas on the particle. It should be noted that we neglect particle-particle interactions in the conservation of momentum. The conservation of energy is

$$\rho^s \frac{d}{dt} \nu' \left(e^{s'} + \frac{u_i' u_i'}{2}\right) = u_i' \int_P \sigma_{ik}' n_k dA_P$$

$$+ \rho^s \nu' g_i u_i' + \int_P \rho^s \left(e^{s'}\right.$$

$$\left. + \frac{u_i' u_i'}{2}\right) \left(v_k^b - u_k'\right) n_k dA_P - \int_P q_i^{s'} n_i dA_P$$

In these equations the derivative d/dt is understood to be Lagrangian. The variables $\rho^s$, $u_i'$, $e^{s'}$, $\nu'$, $q_i^{s'}$, are, respectively, the solid particle density, velocity, specific internal energy, volume and heat flux. If we multiply these equations by $g|x_i - y_i|$ where $y_i$ is the particle location and sum over all particles, we obtain conservation equations for the solid phase. These latter relationships are

$$\rho^s \left\{\frac{\partial}{\partial t} (1-\phi) + \frac{\partial}{\partial x_j} (1-\phi) u_i\right\} = -S \qquad \text{(C.17)}$$

$$\rho^s \left\{\frac{\partial}{\partial t} (1-\phi) u_i + \frac{\partial}{\partial x_j} (1-\phi) u_i u_j\right\} = - \frac{\partial R_{ij}^s}{\partial x_j}$$

$$+ \rho^s (1-\phi) g_i - M_i \qquad \text{(C.18)}$$

$$\rho^s \left\{ \frac{\partial}{\partial t} (1-\phi) \left( e^s + \frac{u_i u_i}{2} \right) + \frac{\partial}{\partial x_j} (1-\phi) u_j \left( e^s + \frac{u_i u_i}{2} \right) \right\}$$

$$+ \frac{\partial}{\partial t} \frac{R^s_{kk}}{2} + \frac{\partial E^s_j}{\partial x_j} = - \frac{\partial}{\partial x_j} u_i R^s_{ij} - N$$

$$+ \rho^s (1-\phi) u_i g_i \qquad \text{(C.19)}$$

where

$$R^s_{ij} = \sum_P \rho^s u_i'' u_j'' v' \; g|x_k - y_k|$$

$$E^s_j = \sum_P \rho^s \left\{ e^{s''} u_j'' + u_i'' u_i'' u_j'' \right\} v' \; g|x_k - y_k|$$

In the equations (C.17)-(C.19), as well as in (C.11)-(C.13), we have implicitly assumed that there is a reaction front propagating into the solid particle. This reaction front moves with the velocity $v_i^b$ and consequently this front locally separates the solid and gas phases. Further, conservation of mass, momentum and energy flux are assumed, and are represented by surface integrals for mass flux, S, momentum flux, $M_i$, and energy flux, N, in the respective spatial averages of the point differential equations (C.11)-(C.13) and (C.17)-(C.19); we summarize these integrals

$$S = - \sum_P \int_P \rho' (v_j^b - v_j') \, n_j \, g \, (|x_k - y_k|) \, dAp \qquad \text{(C.20a)}$$

$$M_i = - \sum_P \int_P \left\{ \rho' v_i' \, (v_j^b - v_j') + \sigma_{ij}' \right\} n_j \, g \, (|x_k - y_k|) \, dA_p \qquad \text{(C.20b)}$$

$$N = - \sum_{P} \int_{P} \left\{ \rho' \left( e' + \frac{v_i' v_i'}{2} \right) (v_j^b - v_j') + v_i' \sigma_{ij}' - q_j' \right\} n_j g \; (|x_k - y_k|) dA_p \qquad \text{(C.20c)}$$

In analogy to the case of slow combustion fronts in gases we can assume that the momentum integral, $M_i$, is dominated by the stress tensor, thereby assuring that continuity of stress occurs at the particle surface. Consistent with that assumption we would also neglect the flux of kinetic energy in the energy integral, N. Again, the surface integrals (C.20) must be defined in terms of averaged variables to provide closure.

NEGLECT OF FLUCTUATIONS

If we neglect products of fluctuations in the averaged equations, they can be simplified considerably.

$$R_i = R_{ij} = E = E_j = 0 \qquad \text{(C.21a)}$$

$$R_{ij}^s = E_j^s = 0 \qquad \text{(C.21b)}$$

With these relationships (C.20) and (C.21), the conservation equations (C.11)-(C.13) and (C.17)-(C.19) become

$$\frac{\partial}{\partial t} \phi \rho_\alpha + \frac{\partial}{\partial x_j} \phi \rho_\alpha v_j = S_\alpha \qquad (\alpha = 1 \ldots) \qquad \text{(C.22a)}$$

$$\frac{\partial}{\partial t} \rho^s (1-\phi) + \frac{\partial}{\partial x_j} \rho^s (1-\phi) u_j = - S \qquad \text{(C.22b)}$$

$$\frac{\partial}{\partial t} \phi \rho v_i + \frac{\partial}{\partial x_j} \phi \rho v_i v_j = \frac{\partial \sigma_{ij}}{\partial x_j} + \phi \rho g_i + M_i \qquad \text{(C.22c)}$$

$$\frac{\partial}{\partial t} \rho^s (1-\phi) u_i + \frac{\partial}{\partial x_j} \rho^s (1-\phi) u_i u_j$$

$$= \rho^s (1-\phi) g_i - M_i \tag{C.22d}$$

$$\frac{\partial}{\partial t} \phi\rho \left(e + \frac{v_i v_i}{2}\right) + \frac{\partial}{\partial x_j} \phi\rho v_j \left(e + \frac{v_i v_i}{2}\right) = \frac{\partial v \sigma_{ij}}{\partial x_j}$$

$$- \frac{\partial \phi q_j}{\partial x_j} + \phi\rho v_i g_i + N \tag{C.22e}$$

$$\frac{\partial}{\partial t} (1-\phi)\ \rho^s \left(e^s + \frac{u_i u_i}{2}\right) + \frac{\partial}{\partial x_j} (1-\phi)\ \rho^s u_j \left(e^s + \frac{u_i u_i}{2}\right)$$

$$= (1-\phi) \rho^s u_i g_i - N \tag{C.22f}$$

Finally, (C.22) must be supplemented by constitutive relationships and chemistry to define the functions $S_\alpha$, $S$, $M_i$, $N$, $q_i$, $\sigma_{ij}$, $e$, $e^s$. Within this context some representation of particle size distribution is clearly required.

We note that (C.22) are analogous to existing equations for multiphase flows. For example, if the interphase mass exchange is neglected and we write

$$\sigma_{ij} = -P\delta_{ij} + \left\{\lambda \frac{\partial v_k}{\partial x_k} + \mu \left[\frac{\partial v_i}{\partial x_j} + \frac{\partial v_j}{\partial x_i} - \frac{2}{3} \delta_{ij} \frac{\partial v_k}{\partial x_k}\right]\right\} \tag{C.23}$$

then (C.22) are essentially the same as Marble's[19] equations for particle laden gas flows. However, while we neglect particle-particle interactions (and also fluctuations) we do not assume that the volume occupied by the particles is negligible.

A multiphase model for condensation and evaporation of droplets in a steady gas flow has been developed by Edelman, *et al.*[20] The source terms in that model, for a single species, retaining the momentum and kinetic energy fluxes associated with interphase mass exchange are

$$S,$$

$$M_i = Su_i - f_i$$

and

$$N = \left(h(T^s) + \frac{u_i u_i}{2}\right) S - Q$$

$$= \left(h^s + L + \frac{u_i u_i}{2}\right) S - Q$$

In these equations $f_i$ and $Q$ are particle-gas drag force and heat transfer, respectively, where the summation is indicated in (C.20). Also, $h^s$ is the enthalpy of the condensed phase at particle temperature $T^s$ and $L$ is the heat of vaporization. In these latter expressions, we have assumed that the particle velocity and temperature are the same as, respectively, the mean solid velocity and temperature. Further, we have assumed that the work term c.f. (C.20)] $v_i' \sigma_{ij}' n_j$, at the particle, is dominated by the hydrostatic pressure.

## CLOSING REMARKS

For the case of entrained flows of a single particle size without chemical reaction or interphase mass exchange, we may use (C.22) and (C.23) to describe the conservation of mass, momentum and energy with

$$\begin{gathered} S = 0 \\ M_i = -f_i, \quad N = -Q \end{gathered} \qquad \text{(C.24)}$$

Also it is unlikely that heat conduction in the gas is important

$$q_j = 0 \tag{C.25}$$

We can assume that the equation of state for the gas phase is

$$P_\alpha = \rho_\alpha \frac{RT}{M_\alpha}, \qquad P = \sum_\alpha P_\alpha \tag{C.26}$$

so we have

$$de_\alpha = C_{V\alpha} dT, \qquad e = \sum_\alpha \frac{\rho_\alpha}{\rho} e_\alpha \tag{C.27}$$

Further, the internal energy of the solid is related to the temperature of the solid by

$$de^s = C_V^s dT^s \tag{C.28}$$

Finally, to close the system of equations, we require a specification of $f_i$ and Q. We expect that such relationships have the form (c.f. Marble[19]),

$$f_i = F_D\ (\phi,\mu,\rho,\rho^s,\nu',\{v_i-u_i\},\ v_i,\ u_i) \tag{C.29}$$

$$Q = F_Q\ (\phi,\mu,\rho,\rho^s,\nu',k,\{T-T^s\},\ T,\ T^s) \tag{C.30}$$